Supporting on-line material for: Topologically protected conduction state at carbon foam surfaces: An *ab-initio* study

Zhen Zhu, Zacharias G. Fthenakis, Jie Guan, and David Tománek*

I. ELECTRONIC STRUCTURE RESULTS FOR THICK FOAM SLABS

As a counterpart to results for thin carbon foam slabs in the main manuscript, we present in the following results for thicker carbon foam structures. The optimized structure of sp^3- and sp^2-terminated $n-$honeycomb thick slabs with $n = 3, 5, 7$ is shown in Fig. S1. The slab surfaces are the same as for the thinner slabs in the main manuscript. Unlike in the thin slabs, sp^2 sites are both at the surface and in the bulk of these thick slabs.

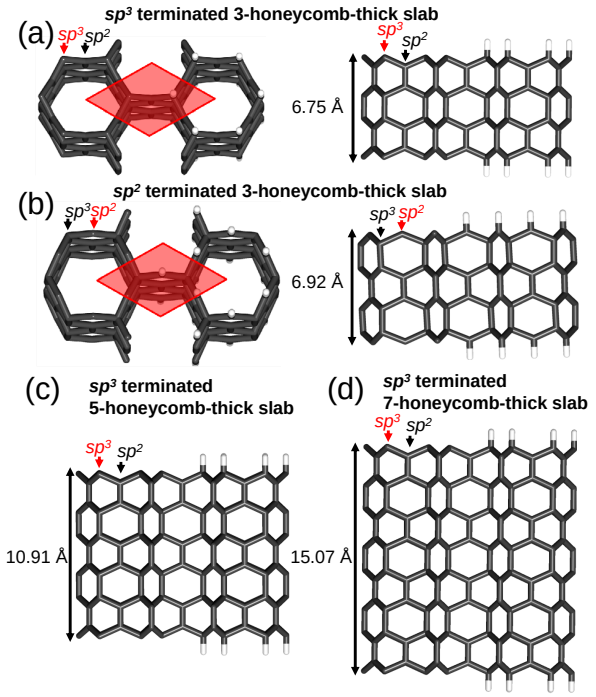

FIG. S1. Optimum geometry of (a) sp^3- and (b) sp^2-terminated 3-honeycomb thick foam slabs. The tilted view in left panels depicts the structure and primitive unit cells. The right panels are side views of the structure that better illustrate the type of termination and illustrate partial hydrogen coverage. Side view of the geometry of sp^3-terminated (c) 5-honeycomb thick and (d) 7-honeycomb thick foam slabs.

The electronic structure and quantum transport in these thicker slabs are presented in Fig. S2. In comparison to our Density Functional Theory (DFT) band structure results for a thin sp^3-terminated slab in the main manuscript, our corresponding result in Fig. S2(a) indicates a much narrower band gap. In reality, this band gap becomes slightly negative as a common DFT-related artifact. A much better representation of band gaps may be obtained by GW or by the HSE hybrid functional[1] calculations mentioned in the following. These calculations, as well as parameterized LCAO calculations,[2] show this structure to be a semiconductor, same as the bulk.

Similar to the thin slabs discussed in the main manuscript, the conduction states in the sp^2-terminated 3-honeycomb thick slab, shown in Fig. S2(c), have $p_{||}$ character. In the thicker slabs, it is clearer that the conduction states are associated with sp^2 sites at the surface only. Thus, the conduction mechanism is caused by the presence of a particular surface and unrelated to the fact that our calculations were performed for finite-thickness slabs.

Our transport results in Fig. S2(d) show that also the sp^2-terminated thick slabs are highly conductive, whereas the sp^3-terminated slabs display a vanishing transport gap linked to the DFT band structure.

The connectivity diagram in Fig. S2(e) illustrates the presence of sp^2 sites in the interior of thick slabs and can be used to explain the conduction in these systems along the arguments used in the main manuscript.

The evolution of the electronic band structure with increasing foam slab thickness is shown in Fig. S3(a-d). With increasing slab thickness, the electronic structure is approaching that of the bulk material, shown in Fig. S3(e).

II. RELIABILITY OF DFT BAND STRUCTURE RESULTS

Electronic band structure results obtained by DFT must be interpreted very carefully. Even though this approach generally underestimates the fundamental band gap, the electronic structure of the valence and the conduction band region is believed to closely represent experimental results. Also in carbon foam, the DFT band gaps become too small and even turn negative in the bulk system, placing the bottom of the conduction band below the top of the valence band. While this is not a point of central interest in our study, we should at least note that a better description of the band gaps may be obtained at substantial computational cost by performing calculations using the HSE hybrid functional[1] or self-energy calculations using the GW approach. Our HSE band structure results, presented in Fig. S3(f), show a fundamental A–H band gap of 0.5 eV. The size of the band gap is consistent with results of our GW calculations us-

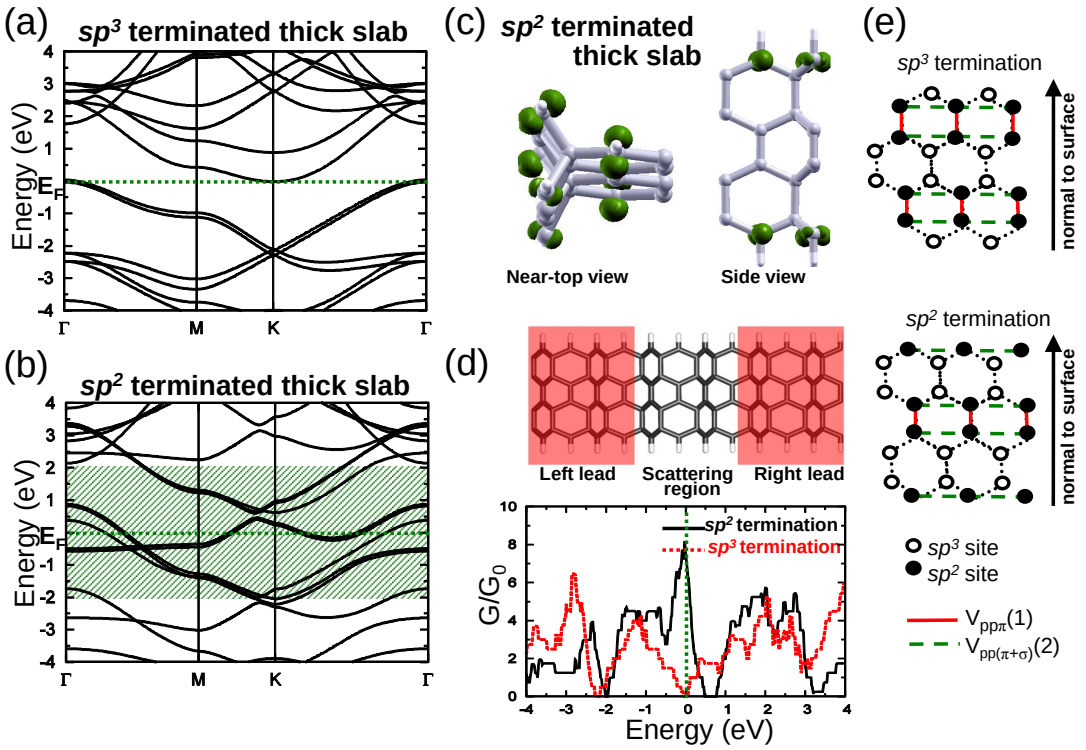

FIG. S2. Electronic structure of 3-honeycomb thick foam slabs. DFT-based band structure of a 3-honeycomb thick, hydrogen-covered foam slab with (a) sp^3 and (b) sp^2 termination on both sides. (c) Charge distribution in the sp^2-terminated slab corresponding to states in the energy range $E_F - 2$ eV$< E < E_F + 2$ eV, indicated by shading in (b). (d) Conductance G of sp^3- and sp^2-terminated slabs in units of the conduction quantum G_0. (e) Connectivity diagram of sp^3- and sp^2-terminated 3-honeycomb thick slabs.

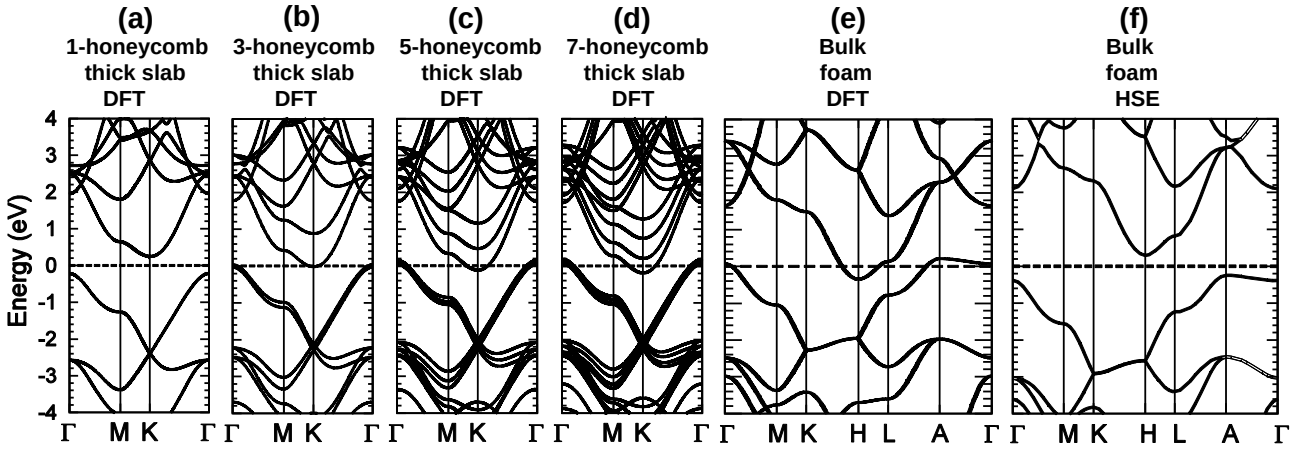

FIG. S3. Electronic band structure of sp^3-terminated foam slabs and of bulk carbon foam. DFT-based band structure is presented for (a) a 1-honeycomb thick, (b) a 3-honeycomb thick, (c) a 5-honeycomb thick, (d) a 7-honeycomb thick slab, and (e) for the bulk structure. (f) Band structure based on the HSE hybrid functional.

ing the Vienna *Ab initio* Simulation Package (VASP).[3] Comparison of our DFT and HSE results in Figs. S3(e) and S3(f) shows that the bulk carbon foam, according to HSE, is a semiconductor, and that the band gap reduction in DFT is an artifact of that approach.

III. EFFECT OF HYDROGEN ADSORPTION ON THE ELECTRONIC STRUCTURE OF CARBON FOAM SLABS AND SURFACES

The electronic structure of bare and hydrogen-covered sp^3- and sp^2-terminated 1-honeycomb thick foam slabs

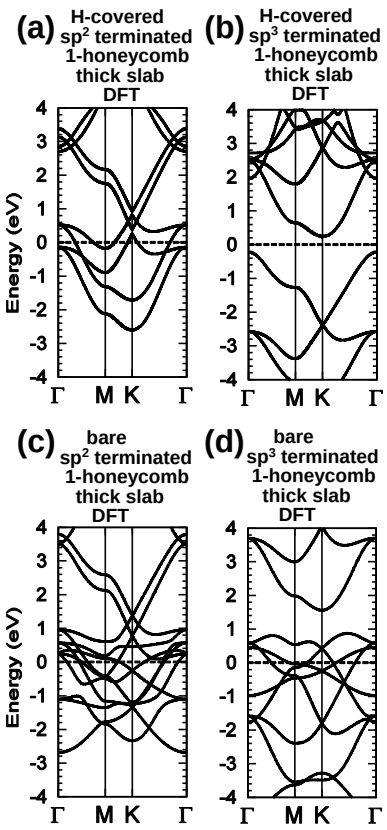

FIG. S4. Comparison between the electronic band structure of (a-b) hydrogen-covered and (c-d) bare sp^2- and sp^3-terminated 1-honeycomb thick foam slabs.

is shown in Fig. S4. On bare surfaces, unsaturated bonds give rise to new conducting states near the Fermi level, as seen in Fig. S4(c-d). These states associated with unsaturated bonds are quenched by hydrogen adsorption. Whereas hydrogen coverage turns the sp^3-terminated surface semiconducting, as seen in Fig. S4(b), a topologically protected conduction state persists at the sp^2-terminated hydrogen covered surface, as seen in Fig. S4(a).

IV. IN-PLANE CONDUCTION ANISOTROPY AT HYDROGEN-COVERED FOAM SURFACES

Results of our quantum transport calculations along different directions on hydrogen-covered sp^3- and sp^2-terminated 1-honeycomb thick foam slabs are shown in Fig. S5. To judge the level of anisotropy, the infinite slab can be thought to be subdivided into strips of constant width, aligned with the transport direction. The fact that conductance results along the armchair and the zigzag direction are nearly the same strongly suggests that the conductance along the foam surface is nearly isotropic.

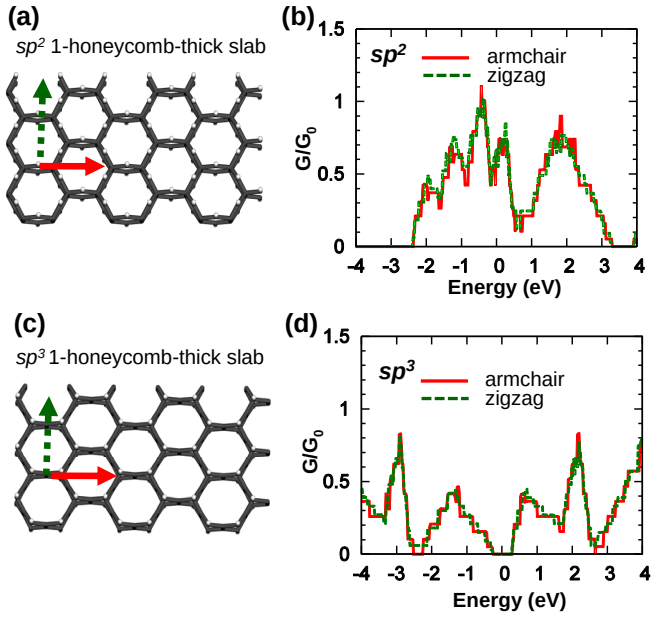

FIG. S5. Tilted view of (a) an sp^2- and (c) an sp^3-terminated foam slab, indicating the armchair and the zigzag direction along the surface. Conduction along the armchair and the zigzag direction in (b) an sp^2- and (d) an sp^3-terminated 1-honeycomb thick foam slab.

V. LINEAR COMBINATION OF ATOMIC ORBITALS (LCAO) HAMILTONIAN

Electronic structure obtained using the LCAO Hamiltonian may provide a better representation of the band gaps than the *ab initio* DFT approach when using adequate parameters. The unique flexibility of the LCAO approach allows to link particular features of the band structure to values associated with interactions between s and p states as well as their on-site energies. We used $E_s = -7.3$ eV and $E_p = 0.0$ eV for the carbon on-site energies and Slater-Koster hopping integrals[4] with a d^{-2} distance dependence between orthogonal orbitals. Their values[5] at the nearest-neighbor distance in diamond $d_1 = 1.546$ Å are $V_{ss\sigma}(d_1) = -3.63$ eV, $V_{sp\sigma}(d_1) = 4.20$ eV, $V_{pp\sigma}(d_1) = 5.38$ eV, and $V_{pp\pi}(d_1) = -2.24$ eV. These values are close to other orthogonal LCAO schemes[6] and were used successfully for a wide range of electronic structure studies.[7,8] We use the values recommended in Ref. 6 for the second-neighbor hopping integrals. The values at the second-neighbor distance in diamond $d_2 = 2.525$ Å are $V_{ss\sigma}(d_2) = 0.14$ eV, $V_{sp\sigma}(d_2) = -0.02$ eV, $V_{pp\sigma}(d_2) = 0.63$ eV, and $V_{pp\pi}(d_2) = -0.24$ eV. Their distance-dependence is $V_{ss\sigma}(d) \sim d^{-1}$, $V_{sp\sigma}(d) \sim d^{-2}$. $V_{pp\sigma}(d) \sim d^{-3}$, and $V_{pp\pi}(d) \sim d^{-3}$.

Hydrogen atoms were described by their on-site energy $\tilde{E}_s(\mathrm{H}) = -2.30$ eV and their interaction with carbon by hopping integrals with a d^{-2} distance dependence.[9] We used $\tilde{V}_{ss\sigma}(d_{\mathrm{CH}}) = -3.15$ eV and $\tilde{V}_{sp\sigma}(d_{\mathrm{CH}}) = 1.70$ eV at the C-H distance $d_{\mathrm{CH}} = 1.07$ Å.

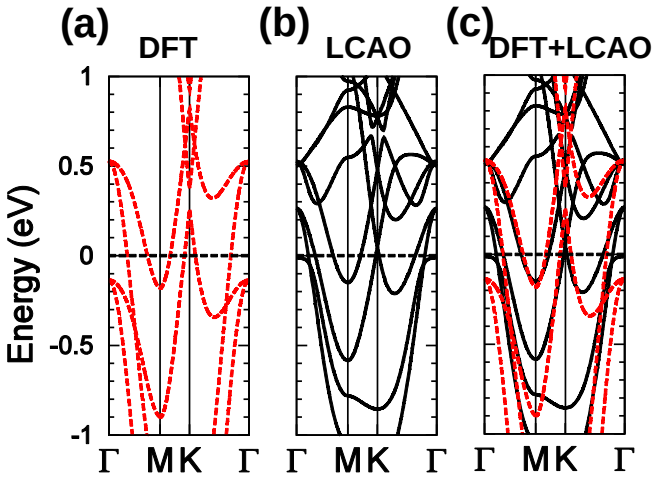

FIG. S6. Comparison between band structure results of an sp^2-terminated, hydrogen covered 1-honeycomb thick slab, obtained using different approaches. (a) DFT results, (b) LCAO results, and (c) their superposition in a 2-eV wide energy range around the Fermi level.

VI. COMPARISON BETWEEN BAND STRUCTURES BASED ON THE *AB* INITIO DFT AND THE PARAMETRIZED LCAO APPROACH

To prove the adequacy of our simplified LCAO approach, which we use to interpret electronic structure results, we present the band structure of an sp^2-terminated, hydrogen covered 1-honeycomb thick slab based on the DFT and the LCAO approach in Fig. S6. Whereas the agreement is not prefect, the most important band features close to E_F are well reproduced. While parametrized, LCAO calculations do not suffer from the band gap reduction in semiconductors as DFT calculations do.

* E-mail: tomanek@pa.msu.edu

[1] J. Heyd, G. E. Scuseria, and M. Ernzerhof, J. Chem. Phys. **118**, 8207 (2003).
[2] A. Kuc and G. Seifert, Phys. Rev. B **74**, 214104 (2006).
[3] G. Kresse and J. Furthmüller, Phys. Rev. B **54**, 11169 (1996).
[4] J. C. Slater and G. F. Koster, Phys. Rev. **94**, 1498 (1954).
[5] D. Tomanek and M. A. Schluter, Phys. Rev. Lett. **67**, 2331 (1991).
[6] D. A. Papaconstantopoulos, ed., *Handbook of the band structure of elemental solids* (Plenum Press, New York and London, 1986).
[7] M. Schluter, M. Lannoo, M. Needels, G. A. Baraff, and D. Tomanek, Phys. Rev. Lett. **68**, 526 (1992).
[8] Y.-K. Kwon, S. Saito, and D. Tomanek, Phys. Rev. B **58**, R13314 (1998).
[9] Y. Wang, G. F. Bertsch, and D. Tomanek, Z. Phys. D **25**, 181 (1993).